

THERMO-DIFFUSION AND DIFFUSION-THERMO EFFECTS ON MHD CONVECTIVE FLOW PAST AN IMPULSIVELY STARTED VERTICAL PLATE EMBEDDED IN POROUS MEDIUM

©Kangkan Choudhury*, Sweety Sharma, Shahir Ahmed

Department of Mathematics, University of Science and Technology Meghalaya, India

*Corresponding Author e-mail: kangkan22@gmail.com

Received March 27, 2024; revised April 15, 2024; April 30, 2024

This study introduces an analytical solution for the unsteady MHD free convection and mass transfer flow past a vertical plate embedded in porous medium, taking into account the Soret and Dufour effects. Initially, the perturbation method is employed to decouple the equations resulting from the coupling of the Soret and Dufour effects. Subsequently, the Laplace Transform Technique is applied to solve the governing equations. The expressions for velocity, temperature, concentration, skin-friction, Nusselt, and Sherwood numbers are derived. The effects of the main parameters are discussed, revealing that an increase in the Soret number leads to a decrease in temperature while increasing velocity and concentration. Similarly, the Dufour parameter causes an increase in temperature and velocity, while concentration decreases. However, the effect of the Dufour and Soret parameters on velocity does not show a significant difference.

Keywords: MHD; Soret effect; Dufour effect; Perturbation; Laplace Transform

PACS: 44.25.+f

1. INTRODUCTION

Environmental and mass transfer are very important in many mechanical systems used directly in processes, solar collectors, nuclear reactor heating, etc. [1-10]. Many studies have been conducted on temperature-induced and concentration-induced flow behavior [11-18]. Convection is more important when concentration and temperature interact simultaneously. In 1879, Charles Soret [19] conducted an experiment in which he discovered that the temperature of a salt mixture in a tube was different and not the same at its two ends. The salt concentration near the edge of the cryogenic tube is higher than that near the high temperature end. This led him to conclude that the decrease in minerals was caused by changes in temperature. This is called the Sorét effect or thermophoresis. However, when heat transfer occurs due to a concentration gradient, the phenomenon is called the Dufour effect. Both of these effects are significant in flow systems where density variations exist, such as during isotope separation, chemical processing, etc. [20-26]. Kafoussias and Williams [27] observed that when heat and mass transfer occur simultaneously in a moving fluid, there will always be a complex relationship between the flow and the driving force. This result was obtained after studying the influence of Soret and Dufour on the constant heat and mass transfer near the boundary layer with mixed forced free convection. Their conclusion was that concentration gradients can also create energy flow. Using HAM, the authors [28] solved the system of equations governing steady 2D flow through a long moving porous wall containing conductive fluid in a permeable medium. The authors in [29] presented an analytical study of the Soret and Dufour effects of a second-quality fluid flow along an elongated cylinder taking into account the influence of thermal radiation. It is expected that when the Soret and Dufour parameters change simultaneously, the heat and mass transfer rates will have an inverse relationship with each other.

MHD is a branch of physics that studies the behavior of fluids in magnetic fields. MHD liquids flowing through pipelines are of great significance in many scientific and technical fields such as bioengineering, petroleum industry, drainage and irrigation. The application of MHD principle is widely used in fusion reactors, MHD pump design, MHD generators, MHD speedometers, etc. MHD principles are also used in medicine and biology. Alfven [30], Cowling [31], Shercliff [32], Crammer and Pai [33] are other notable authors whose contributions have led to the development of MHD to its present form. Jha and Gambo [34] used an analytical approach to study inelastic flow and mass transfer on fixed plates by Soret and Dufour. The author first uses the perturbation method to simplify the system of equations, and then uses the Laplace transform technique to solve the system of equations.

The main objective of the present investigation is to present comprehensive analytical solutions for unsteady MHD-free convection and mass transfer on a vertical plate impulsively moved and embedded in a porous medium in the presence of aspect of the Soret and Dufour effects. The coupled equations of the temperature and concentration fields are decoupled using perturbation techniques and then solved by applying the Laplace transform technique. The present work generalizes the work done by [34] by introducing a magnetic field and considering the porosity of the medium. The results presented here are compared with the existing literature in which the magnetic and porosity parameters are not available. The solution of Jha and Gambo [34] is given as a special case in the absence of magnetic and porosity parameters.

2. MATHEMATICAL ANALYSIS

The MHD unsteady natural convection flow beyond the pulse-initiated vertical plate embedded in the porous medium is considered. The y -axis is taken along the normal line of the plate and the x -axis is parallel to it. Initially at

$t' \leq 0$, the liquid and the plate are considered to be at rest with the same constant temperature (T'_∞) and concentration (C'_∞). At $t' > 0$, the plate starts moving with a vertical velocity U_0 and the fluid, temperature, and concentration at the plate are maintained at T'_w and C'_w , respectively. All physical quantities depend on t' and y' only because the plate occupying the plane $y' = 0$ is considered to be of infinite length.

The equations governing the flow under such assumptions and Boussinesq approximation in the presence of magnetic field are:

$$\frac{\partial u'}{\partial t'} = \nu \frac{\partial^2 u'}{\partial y'^2} + g\beta(T' - T'_\infty) + g\bar{\beta}(C' - C'_\infty) - \frac{\sigma B_0^2 u'}{\rho} - \frac{\nu u'}{K'}, \tag{1}$$

$$\frac{\partial T'}{\partial t'} = \alpha \frac{\partial^2 T'}{\partial y'^2} + D^* \frac{\partial^2 C'}{\partial y'^2}, \tag{2}$$

$$\frac{\partial C'}{\partial t'} = D_M \frac{\partial^2 C'}{\partial y'^2} + S^* \frac{\partial^2 T'}{\partial y'^2}. \tag{3}$$

Subject to

$$t' \leq 0: u' = 0, T' = T'_\infty, C' = C'_\infty \text{ for } y' \geq 0, \tag{4}$$

$$t' > 0: \begin{cases} u' = U_0, T' = T'_w, C' = C'_w \text{ at } y' = 0 \\ u' \rightarrow 0, T' \rightarrow T'_\infty, C' \rightarrow C'_\infty \text{ as } y' \rightarrow \infty \end{cases} \tag{5}$$

While the following non-dimensional quantities are introduced

$$u = \frac{u'}{U_0}, y = \frac{y' U_0}{\nu}, t = \frac{t' U_0^2}{\nu}, \theta = \frac{T' - T'_\infty}{T'_w - T'_\infty}, \phi = \frac{C' - C'_\infty}{C'_w - C'_\infty},$$

$$G_T = \frac{\nu g \beta (T'_w - T'_\infty)}{U_0^3}, G_M = \frac{\nu g \bar{\beta} (C'_w - C'_\infty)}{U_0^3}, Pr = \frac{\nu}{\alpha}, S_c = \frac{\nu}{D_M},$$

$$M = \frac{\sigma B_0^2 \nu}{\rho U_0^2}, K_p = \frac{K' U_0^2}{\nu^2}, D_u = \frac{D^* (C'_w - C'_\infty)}{(T'_w - T'_\infty)}, S_r = \frac{D^* (T'_w - T'_\infty)}{(C'_w - C'_\infty)}, \xi = M + \frac{1}{K_p}.$$

Where Pr is the Prandtl number, S_c the Schmidt number, G_T the Grashof number, G_M the modified Grashof number, M the magnetic parameter, K_p the permeability parameter, S_r the Soret parameter and D_u is the Dufour parameter in Eqs (1-3), we get

$$\frac{\partial u}{\partial t} = \frac{\partial^2 u}{\partial y^2} + G_T \theta + G_M \phi - \xi u, \tag{6}$$

$$\frac{\partial \theta}{\partial t} = \frac{1}{Pr} \frac{\partial^2 \theta}{\partial y^2} + \frac{D_u}{Pr} \frac{\partial^2 \phi}{\partial y^2}, \tag{7}$$

$$\frac{\partial \phi}{\partial t} = \frac{1}{S_c} \frac{\partial^2 \phi}{\partial y^2} + \frac{S_r}{S_c} \frac{\partial^2 \theta}{\partial y^2}. \tag{8}$$

Subject to the following initial and boundary conditions

$$t \leq 0: u = 0, \theta = 0, \phi = 0 \text{ for } y \geq 0, \tag{9}$$

$$t > 0: \begin{cases} u = 1, \theta = 1, \phi = 1 \text{ at } y = 0 \\ u \rightarrow 0, \theta \rightarrow 0, \phi \rightarrow 0 \text{ as } y \rightarrow \infty \end{cases} \tag{10}$$

3. ANALYTICAL SOLUTIONS

In order to solve the coupled equations (6 - 8) analytically, we use a non-zero parameter ε (sufficiently small) in the following form, so that the equations are decoupled:

$$u = u_0 + \varepsilon u_1 + O(\varepsilon^2), \tag{11}$$

$$\theta = \theta_0 + \varepsilon\theta_1 + O(\varepsilon^2), \quad (12)$$

$$\phi = \phi_0 + \varepsilon\phi_1 + O(\varepsilon^2). \quad (13)$$

Here $D_u = k\varepsilon$, $S_r = \lambda\varepsilon$

and k , λ are constants of $O(1)$. Then substituting (11 - 13) into (6 - 10) gives:

3.1 Order ε^0

$$\frac{\partial u_0}{\partial t} = \frac{\partial^2 u_0}{\partial y^2} + G_T \theta + G_M \phi - \xi u_0, \quad (14)$$

$$\frac{\partial \theta_0}{\partial t} = \frac{1}{\text{Pr}} \frac{\partial^2 \theta_0}{\partial y^2}, \quad (15)$$

$$\frac{\partial \phi_0}{\partial t} = \frac{1}{S_c} \frac{\partial^2 \phi_0}{\partial y^2}, \quad (16)$$

$$u_0(y, t) = 1, \theta_0(y, t) = 1, \phi_0(y, t) = 1 \text{ at } y = 0, \quad (17)$$

$$u_0(y, t) = 0, \theta_0(y, t) = 0, \phi_0(y, t) = 0 \text{ as } y \rightarrow \infty. \quad (18)$$

3.2. Order ε^1

$$\frac{\partial u_1}{\partial t} = \frac{\partial^2 u_1}{\partial y^2} + G_T \theta + G_M \phi - \xi u_1, \quad (19)$$

$$\frac{\partial \theta_1}{\partial t} = \frac{1}{\text{Pr}} \frac{\partial^2 \theta_1}{\partial y^2} + \frac{k}{\text{Pr}} \frac{\partial^2 \phi_0}{\partial y^2}, \quad (20)$$

$$\frac{\partial \phi_1}{\partial t} = \frac{1}{S_c} \frac{\partial^2 \phi_1}{\partial y^2} + \frac{\lambda}{\text{Pr}} \frac{\partial^2 \theta_0}{\partial y^2}, \quad (21)$$

$$u_1(y, t) = 0, \theta_1(y, t) = 0, \phi_1(y, t) = 0 \text{ at } y = 0, \quad (22)$$

$$u_1(y, t) = 0, \theta_1(y, t) = 0, \phi_1(y, t) = 0 \text{ as } y \rightarrow \infty. \quad (23)$$

Using Laplace Transform Technique with relevant boundary conditions, the solutions are obtained as

$$\theta(y, t) = P_2 \text{erfc} \left(\frac{y}{2} \sqrt{\frac{\text{Pr}}{t}} \right) - P_1 \text{erfc} \left(\frac{y}{2} \sqrt{\frac{S_c}{t}} \right), \quad (24)$$

$$\phi(y, t) = P_4 \text{erfc} \left(\frac{y}{2} \sqrt{\frac{S_c}{t}} \right) - P_3 \text{erfc} \left(\frac{y}{2} \sqrt{\frac{\text{Pr}}{t}} \right), \quad (25)$$

$$u(y, t) = \left(1 - \frac{Z_1}{a_1} - \frac{Z_2}{a_2} \right) f_1 + \frac{Z_1}{a_1} \text{erfc} \left(\frac{y}{2} \sqrt{\frac{\text{Pr}}{t}} \right) + \frac{Z_2}{a_2} \text{erfc} \left(\frac{y}{2} \sqrt{\frac{S_c}{t}} \right) + \frac{Z_1}{a_1} e^{a_1 t} (f_2 - f_3) + \frac{Z_2}{a_2} e^{a_2 t} (f_4 - f_5), \quad (26)$$

where

$$P_1 = \frac{D_u S_c}{S_c - \text{Pr}}, P_2 = 1 + P_1, P_3 = \frac{\text{Pr} S_r}{\text{Pr} - S_c}, P_4 = 1 + P_3, a_1 = \frac{\xi}{\text{Pr} - 1}, a_2 = \frac{\xi}{S_c - 1}$$

$$Z_1 = \frac{G_T (\text{Pr} - S_c) - S_r \text{Pr} G_M - D_u S_c G_T}{(\text{Pr} - 1)(\text{Pr} - S_c)}, Z_2 = \frac{G_M (S_c - \text{Pr}) - S_r \text{Pr} G_M - D_u S_c G_T}{(S_c - 1)(S_c - \text{Pr})}$$

$$f_1 = f(1, \xi, y, t), f_2 = f(1, \xi + a_1, y, t), f_3 = f(\text{Pr}, a_1, y, t)$$

$$f_4 = f(1, \xi + a_2, y, t), f_5 = f(S_c, a_2, y, t)$$

$$f(x, z, y, t) = \frac{1}{2} \left[e^{y\sqrt{z}} \operatorname{erfc} \left(\frac{y}{2} \sqrt{\frac{x}{t} + \sqrt{zt}} \right) + e^{-y\sqrt{z}} \operatorname{erfc} \left(\frac{y}{2} \sqrt{\frac{x}{t} - \sqrt{zt}} \right) \right]$$

The non-dimensional form of Nusselt number, Sherwood number, and skin friction coefficient in heat and mass transfer process as

$$Nu = - \left[\frac{\partial \theta}{\partial y} \right]_{y=0} = -P_1 \sqrt{\frac{S_c}{\pi t}} + P_2 \sqrt{\frac{\text{Pr}}{\pi t}} \tag{27}$$

$$Sh = - \left[\frac{\partial \phi}{\partial y} \right]_{y=0} = -P_3 \sqrt{\frac{\text{Pr}}{\pi t}} + P_4 \sqrt{\frac{S_c}{\pi t}} \tag{28}$$

$$C_f = - \left[\frac{\partial u}{\partial y} \right]_{y=0} = \left(1 - \frac{Z_1}{a_1} - \frac{Z_2}{a_2} \right) \left(\sqrt{\xi} \operatorname{erfc}(\sqrt{\xi t}) + \frac{1}{\sqrt{\pi t}} \right) + \frac{Z_1}{a_1} \sqrt{\frac{\text{Pr}}{\pi t}} + \frac{Z_2}{a_2} \sqrt{\frac{S_c}{\pi t}} - \frac{Z_1}{a_1} e^{a_1 t} g_1 - \frac{Z_2}{a_2} e^{a_2 t} g_2. \tag{29}$$

Where

$$g_1 = g(a_1, \xi + a_1, t), g_2 = g(a_2, \xi + a_2, t), g(x, z, t) = \sqrt{x} \operatorname{erfc}(\sqrt{xt}) - \sqrt{z} \operatorname{erfc}(\sqrt{zt})$$

4. RESULTS AND DISCUSSIONS

The mathematical model describes the free convection flow associated with heat and mass transfer across a vertical plate that initiates pulses in addition to thermal diffusion and thermal-diffusion effects. Numerical calculations were performed to provide an overall understanding of the problem and the results are presented in Figures 1 to 9 and Table 1.

To have a clear overview of the problem, the calculations Numbers for the velocity field, dimensionless temperature and concentration fields, surface friction, heat and mass transfer rates have been taken and they are represented graphically for the thermal Grashof number G_T , the modified Grashof number G_M , Schmidt number S_c , Prandtl number P_r , magnetic parameter M , Soret parameter S_r , Dufour parameter and permeability parameter. The Prandtl P_r number is chosen to be 0.71, representing air at a temperature of 290 K and a pressure of 1 atm. In this study, air is considered as the primary fluid (solvent) and certain fluids are considered as secondary substances (solute) such as helium (He), water vapor (H_2O), ammonia (NH_3), etc. is diffused in the air. The Schmidt number Sc is assumed to be 0.78 typical for ammonia (NH_3), while the values of the other parameters are chosen arbitrarily.

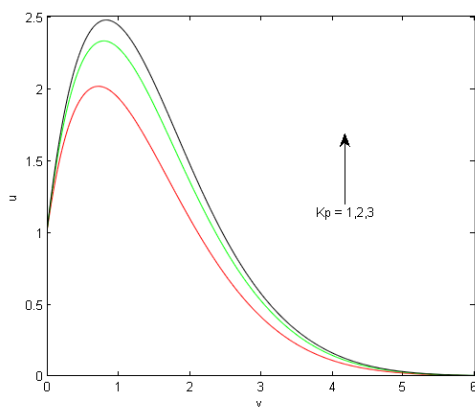


Figure 1. Velocity profile with respect to permeability parameter for $k_p = 1; S_c = 0.78; P_r = 0.71; G_T = 5; G_M = 5; M = 1; t = 1; D_u = 0.15; S_r = 0.15$

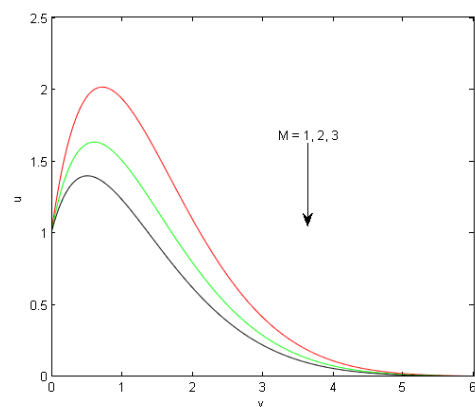


Figure 2. Velocity profile with respect to magnetic parameter for $k_p = 1; S_c = 0.78; P_r = 0.71; G_T = 5; G_M = 5; M = 1; t = 1; D_u = 0.15; S_r = 0.15$

Figure 1 depicts the influence of permeability parameter K_p on the velocity fields. It is found that the velocity increases with increase of permeability parameter K_p for the cooling surface. Physically, when the holes of the porous

medium become large, the resistance of the medium may be neglected and as a consequence the fluid velocity gets increased.

Figure 2 show that velocity decreases comprehensively for increasing Hartmann number. In other words, the fluid flow is decelerated due to imposition of the transverse magnetic field. This observation is consistent with the physical fact that a magnetic body force viz. Lorentz force develops due to interaction of the fluid velocity and the magnetic field which serves as a resistive force to the fluid flow and as a consequence the flow gets decelerated.

The variation in the velocity distribution of the flow field with respect to y for four specific values of Soret parameter (S_r) is shown in Figure 3. It is evident in the figure that the velocity profile diminutions near the plate due to the Soret effect, but at far away from the plate, Soret effect can be used to boost the fluid velocity.

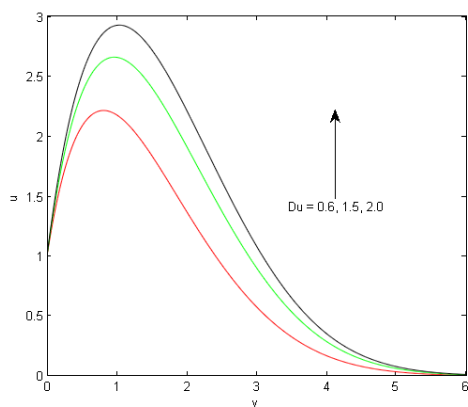


Figure 3. Velocity profile with respect to Dufour parameter for $k_p = 1; S_c = 0.78; P_r = 0.71; G_T = 5; G_M = 5; M = 1; t = 1; D_u = 0.15; S_r = 0.15$

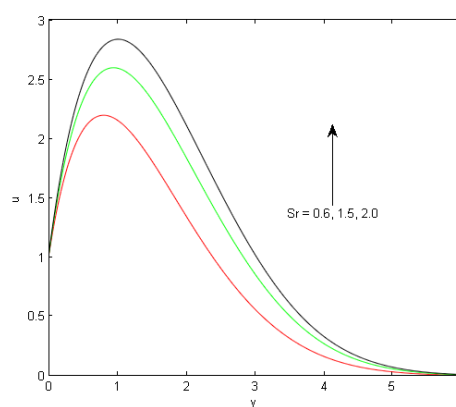


Figure 4. Velocity profile with respect to Soret parameter for $k_p = 1; S_c = 0.78; P_r = 0.71; G_T = 5; G_M = 5; M = 1; t = 1; D_u = 0.15; S_r = 0.15$

The consequences of diffusion-thermo on the velocity field are displayed in Figure 4. The Dufour number D_u signifies the contribution of the concentration gradients to the thermal energy flux in the flow. As D_u increases, a rise in fluid velocity can be seen in Figure 4.

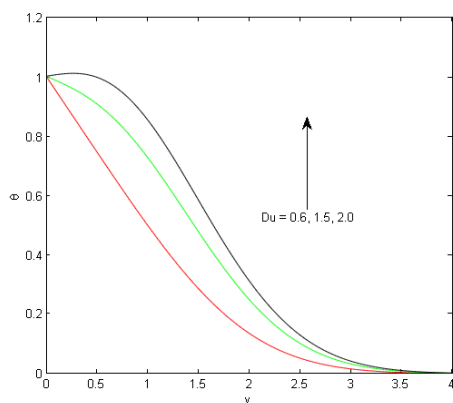


Figure 5. Temperature profile with respect to Dufour parameter for $k_p = 1; S_c = 0.78; P_r = 0.71; G_T = 5; G_M = 5; M = 1; t = 1; D_u = 0.15; S_r = 0.15$

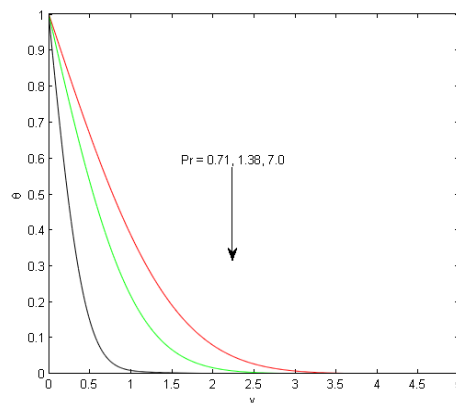


Figure 6. Temperature profile with respect to Prandtl number for $k_p = 1; S_c = 0.78; P_r = 0.71; G_T = 5; G_M = 5; M = 1; t = 1; D_u = 0.15; S_r = 0.15$

Figure 5 illuminates the effect of Prandtl number P_r on fluid temperature. Prandtl number defines the ratio of momentum diffusivity to thermal diffusivity. As P_r increases thermal diffusivity decreases resulting in a drop in fluid temperature. And hence the fluid temperature decreases. Dufour effect on the temperature profile is demonstrated in Figure 6. It is evident that the temperature of the fluid increased with the increasing values of Dufour parameter. Figure 7 indicates the temperature distribution with respect to time. As time progress, temperature of the fluid increases.

In Figure 8, the effect of Schmidt number S_c on concentration field has been depicted. An increase in Schmidt number S_c means a fall in mass diffusivity and hence indicates a fall in the concentration level. Figure 9 presented thermal diffusion effect on concentration profile. It is observed that fluid concentration increased with the increasing values of the Soret parameter S_r . Physically, the presence of thermal diffusion increases the concentration level of the fluid.

From Table 1, as G_T, G_M, K_p increase, skin friction increases. In addition to this, it is seen from Table 1 that the skin friction gets reduced for increasing magnetic parameter M . This indicates that the imposition of a transverse magnetic field inhibits viscous drag due to its application on thin films with high aspect ratio. Henceforth, the coefficient of momentum at the planar surface becomes larger for increasing M . Also, as S_r and D_u increase, viscous drag at the plate decreases.

In Table 2, we have compared our work with previously published work done by [34]. In absence of magnetic parameter and porosity parameter, the variation of skin friction in terms of Soret and Dufour effects are examined. It is found that the findings of the current study are consistent with the prior outcomes.

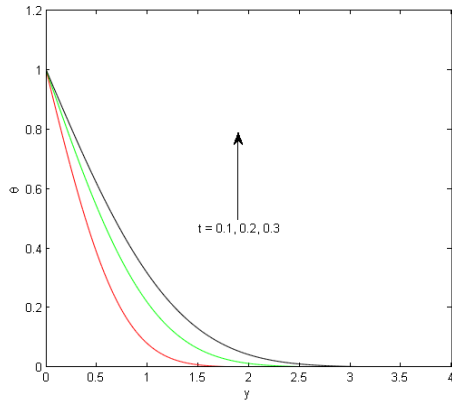


Figure 7. Temperature profile with respect to time for $k_p = 1$; $S_c = 0.78$; $P_r = 0.71$; $G_T = 5$; $G_M = 5$; $M = 1$; $t = 1$; $D_u = 0.15$; $S_r = 0.15$

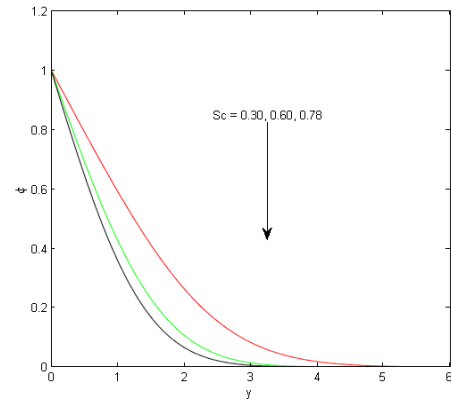


Figure 8. Concentration profile with respect to Schmidt number for $k_p = 1$; $S_c = 0.78$; $P_r = 0.71$; $G_T = 5$; $G_M = 5$; $M = 1$; $t = 1$; $D_u = 0.15$; $S_r = 0.15$

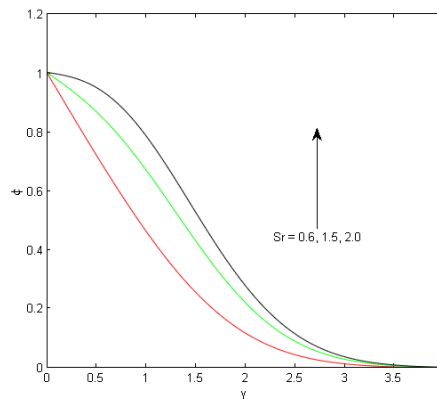


Figure 9. Concentration profile with respect to Soret parameter for $k_p = 1$; $S_c = 0.78$; $P_r = 0.71$; $G_T = 5$; $G_M = 5$; $M = 1$; $t = 1$; $D_u = 0.15$; $S_r = 0.15$

Table 1. Skin friction for the variations of different parameters (M, k_p, S_r, D_u, S_c) for $k_p = 1$; $S_c = 0.78$; $P_r = 0.71$; $G_T = 5$; $G_M = 5$; $M = 1$; $t = 1$; $D_u = 0.15$; $S_r = 0.15$

| M | k_p | D_u | S_r | S_c | τ |
|-----|-------|-------|-------|-------|--------|
| 2 | 1 | 0.15 | 0.15 | 0.78 | 0.8807 |
| 3 | 1 | 0.15 | 0.15 | 0.78 | 0.8673 |
| 4 | 1 | 0.15 | 0.15 | 0.78 | 0.8527 |
| 3 | 1 | 0.15 | 0.15 | 0.78 | 0.8673 |
| 3 | 2 | 0.15 | 0.15 | 0.78 | 0.8749 |
| 3 | 3 | 0.15 | 0.15 | 0.78 | 0.8772 |
| 3 | 1 | 0 | 0.15 | 0.78 | 1.0057 |
| 3 | 1 | 0.15 | 0.15 | 0.78 | 0.8673 |
| 3 | 1 | 0.3 | 0.15 | 0.78 | 0.7788 |
| 3 | 1 | 0.15 | 0 | 0.78 | 0.9879 |
| 3 | 1 | 0.15 | 0.15 | 0.78 | 0.8673 |
| 3 | 1 | 0.15 | 0.3 | 0.78 | 0.7858 |
| 3 | 1 | 0.15 | 0.15 | 0.30 | 1.1474 |
| 3 | 1 | 0.15 | 0.15 | 0.60 | 0.9861 |
| 3 | 1 | 0.15 | 0.15 | 0.78 | 0.8673 |

Table 2: Comparison of the coefficient of skin friction with the previously published work in absence of magnetic parameter (M) and permeability parameter (k_p).

| S_r | D_u | Work done by [34] | τ (Present work) |
|-------------|-------------|-------------------|-----------------------|
| 0.0 | 0.15 | 2.762960 | 2.7615 |
| 0.15 | 0.15 | 2.815850 | 2.8043 |
| 0.3 | 0.15 | 2.869490 | 2.8451 |
| 0.15 | 0.0 | 2.756830 | 2.7458 |
| 0.15 | 0.15 | 2.815850 | 2.8082 |
| 0.15 | 0.3 | 2.875640 | 2.8725 |

5. CONCLUSIONS

In the present investigation, we have studied theoretically the effect of unsteady MHD heat and mass transfer natural fluid flow past an impulsively started vertical plate embedded in porous medium. The present investigation leads to the following conclusions:

- i. Fluid velocity decreases with the increasing values of the magnetic field parameter in the boundary layer region and thus magnetic field can be effectively used in controlling the fluid motion.
- ii. Fluid motion enhances under the effect of Grashof number (G_T) and modified Grashof number (G_M) while the fluid velocity reduced with the increase in Prandtl number and Schmidt number.
- iii. Fluid velocity increases with the increasing values of permeability parameter.
- iv. Fluid velocity increases as Soret (S_r) and Dufour (D_u) number increase.
- v. Temperature of the fluid decreases under the influence of Prandtl number.
- vi. Coefficient of skin-friction of plate is decreased due to the application of the strength of the magnetic field.
- vii. Viscous drag at the plate is increased with the increasing values of permeability parameter.
- viii. Skin friction is decreased with the increasing values of Soret (S_r) and Dufour (D_u) number.

ORCID

©Kangkan Choudhury, <https://orcid.org/0000-0003-2809-8428>

REFERENCES

- [1] N. Marneni, S. Tippa, and R. Pendyala, "Ramp temperature and Dufour effects on transient MHD natural convection flow past an infinite vertical plate in a porous medium," *Eur. Phys. J. Plus.* **130**, 251 (2015). <https://doi.org/10.1140/epjp/i2015-15251-9>
- [2] R. Derakhshan, A. Shojaeia, K. Hosseinzadeh, M. Nimafar, and D.D. Ganji, "Hydrothermal analysis of magneto hydrodynamic nanofluid flow between two parallel by AGM," *Case Stud. Therm. Eng.* **14**, 100439 (2019). <https://doi.org/10.1016/j.csite.2019.100439>
- [3] M.R. Zangoee, Kh. Hosseinzadeh, D.D. Ganji, "Hydrothermal analysis of MHD nanofluid (TiO₂-GO) flow between two radiative stretchable rotating disks using AGM," *Case Stud. Therm. Eng.* **14**, 100460 (2019). <https://doi.org/10.1016/j.csite.2019.100460>
- [4] M. Gholinia, Kh. Hosseinzadeh, H. Mehrzadi, D.D. Ganji, and A.A. Ranjbar, "Investigation of MHD Eyring-Powell fluid flow over a rotating disk under effect of homogeneous-heterogeneous reactions," *Case Stud. Therm. Eng.* **13**, 100356 (2019). <https://doi.org/10.1016/j.csite.2018.11.007>
- [5] M. Gholinia, M. Armin, A.A. Ranjbar, and D.D. Ganji, "Numerical thermal study on CNTs/C₂H₆O₂-H₂O hybrid base nanofluid upon a porous stretching cylinder under impact of magnetic source," *Case Stud. Therm. Eng.* **14**, 100490 (2019). <https://doi.org/10.1016/j.csite.2019.100490>
- [6] M. Gholinia, S. Gholinia, Kh. Hosseinzadeh, and D.D. Ganji, "Investigation on ethylene glycol Nano fluid flow over a vertical permeable circular cylinder under effect of magnetic field," *Results Phys.* **9**, 1525-1533 (2018). <https://doi.org/10.1016/j.rinp.2018.04.070>
- [7] S.M. Mousazadeh, M.M. Shahmardan, T. Tavangar, Kh. Hosseinzadeh, and D.D. Ganji, "Numerical investigation on convective heat transfer over two heated wall-mounted cubes in tandem and staggered arrangement," *Theor. Appl. Mech. Lett.* **8**, 171-183 (2018). <https://doi.org/10.1016/j.taml.2018.03.005>
- [8] S.S. Ghadikolaei, Kh. Hosseinzade, M. Yassari, H. Sadeghi, and D.D. Ganji, "Analytical and numerical solution of non-Newtonian second-grade fluid flow on a stretching sheet," *Therm. Sci. Eng. Prog.* **5**, 309-316 (2018). <https://doi.org/10.1016/j.tsep.2017.12.010>
- [9] S.S. Ardahaie, A.J. Amiri, A. Amouei, K. Hosseinzadeh, and D.D. Ganji, "Investigating the effect of adding nanoparticles to the blood flow in presence of magnetic field in a porous blood arterial," *Inform. Med. Unlocked*, **10**, 71-81 (2018). <https://doi.org/10.1016/j.imu.2017.10.007>
- [10] J. Rahimi, D.D. Ganji, M. Khaki, and Kh. Hosseinzadeh, "Solution of the boundary layer flow of an Eyring-Powell non-Newtonian fluid over a linear stretching sheet by collocation method," *Alex. Eng. J.* **56**, 621-627 (2017). <https://doi.org/10.1016/j.aej.2016.11.006>
- [11] S.S. Ghadikolaei, K. Hosseinzadeh, and D.D. Ganji, "Investigation on Magneto Eyring-Powell nanofluid flow over inclined stretching cylinder with nonlinear thermal radiation and Joule heating effect," *World J. Eng.* **16**, 51-63 (2019). <https://doi.org/10.1108/WJE-06-2018-0204>
- [12] S.S. Ghadikolaei, Kh. Hosseinzade, and D.D. Ganji, "Investigation on ethylene glycol-water mixture fluid suspend by hybrid nanoparticles (TiO₂-CuO) over rotating cone with considering nanoparticles shape factor," *J. Mol. Liq.* **272**, 226-236 (2018). <https://doi.org/10.1016/j.molliq.2018.09.084>

- [13] S.S. Ghadikolaie, Kh. Hosseinzadeh, and D.D. Ganji, "Numerical study on magnetohydrodynamic CNTs-water nanofluids as a micropolar dusty fluid influenced by non-linear thermal radiation and joule heating effect," *Powder Technol.* **340**, 389–399 (2018). <https://doi.org/10.1016/j.powtec.2018.09.023>
- [14] S.S. Ghadikolaie, K. Hosseinzadeh, M. Hatami, and D.D. Ganji, "MHD boundary layer analysis for micropolar dusty fluid containing Hybrid nanoparticles (Cu-Al₂O₃) over a porous medium," *J. Mol. Liq.* **268**, 813–823 (2018). <https://doi.org/10.1016/j.molliq.2018.07.105>
- [15] S.S. Ghadikolaie, Kh. Hosseinzadeh, and D.D. Ganji, "MHD radiative boundary layer analysis of micropolar dusty fluid with graphene oxide (Go)-engine oil nanoparticles in a porous medium over a stretching sheet with joule heating effect," *Powder Technol.* **338**, 425–437 (2018). <https://doi.org/10.1016/j.powtec.2018.07.045>
- [16] S.S. Ghadikolaie, K. Hosseinzadeh, M. Hatami, D.D. Ganji, and M. Armin, "Investigation for squeezing flow of ethylene glycol (C₂H₆O₂) carbon nanotubes (CNTs) in rotating stretching channel with nonlinear thermal radiation," *J. Mol. Liq.* **263**, 10–21 (2018). <https://doi.org/10.1016/j.molliq.2018.04.141>
- [17] S.S. Ghadikolaie, Kh. Hosseinzadeh, and D.D. Ganji, "Investigation on three-dimensional squeezing flow of mixture base fluid (ethyleneglycol–water) suspended by hybrid nanoparticle (Fe₃O₄-Ag) dependent on shape factor," *J. Mol. Liq.* **262**, 376–388 (2018). <https://doi.org/10.1016/j.molliq.2018.04.094>
- [18] S.S. Ghadikolaie, K. Hosseinzadeh, M. Hatami, and D.D. Ganji, "Fe₃O₄-(CH₂OH)₂ nanofluid analysis in a porous medium under MHD radiative boundary layer and dusty fluid," *J. Mol. Liq.* **258**, 172–185 (2018). <https://doi.org/10.1016/j.molliq.2018.02.106>
- [19] J.K. Platten, "The Soret effect: a review of recent experimental results," *J. Appl. Mech.* **73**(1), 5–15 (2006). <https://doi.org/10.1115/1.1992517>
- [20] M.A. Rahman, and M.Z. Saghir, "Thermodiffusion or Soret effect: historical review," *Int. J. Heat Mass. Transf.* **73**, 693–705 (2014). <https://doi.org/10.1016/j.ijheatmasstransfer.2014.02.057>
- [21] M. Bourich, M. Hasnaoui, M. Mamou, et al., "Soret effect inducing subcritical and Hopf bifurcations in a shallow enclosure filled with a clear binary fluid or a saturated porous medium: a comparative study," *Phys Fluids*, **16**, 551–568 (2004). <https://doi.org/10.1063/1.1636727>
- [22] M.S. Malashetty, "Anisotropic thermoconvective effects on the onset of double diffusive convection in a porous medium," *Int. J. Heat Mass. Transf.* **36**, 2397–2401 (1993). [https://doi.org/10.1016/S0017-9310\(05\)80123-1](https://doi.org/10.1016/S0017-9310(05)80123-1)
- [23] R.G. Mortimer, and H. Eyring, "Elementary transition state theory of the Soret and Dufour effects," *Proc. Natl. Acad. Sci. USA*, **77**, 1728–1731 (1980). <https://www.ncbi.nlm.nih.gov/pmc/articles/PMC348577/pdf/pnas00667-0043.pdf>
- [24] G.V.R. Reddy, "Soret and Dufour Effects on MHD free convective flow past a vertical porous plate in the presence of heat generation," *Int. J. Appl. Mech. Eng.* **21**, 649–665 (2016). <https://doi.org/10.1515/ijame-2016-0039>
- [25] K.J. Basant, and O.A. Abiodun, "Free convective flow of heat generating/absorbing fluid between vertical porous plates with periodic heat input," *Int. Commun. Heat Mass.* **36**, 624–631 (2009). <https://doi.org/10.1016/j.icheatmasstransfer.2009.03.003>
- [26] Kh. Hosseinzadeh, M. Alizadeh, and D.D. Ganji, "Hydrothermal analysis on MHD squeezing nanofluid flow in parallel plates by analytical method," *Int. J. Mech. Mater. Eng.* **13**, 4 (2018). <https://doi.org/10.1186/s40712-018-0089-7>
- [27] N.G. Kafoussias, and E.W. Williams, "Thermal-diffusion and diffusion-thermo effects on mixed free-forced convective and mass transfer boundary layer flow with temperature dependent viscosity," *Int. J. Eng. Sci.* **33**, 1369–1384 (1995). [https://doi.org/10.1016/0020-7225\(94\)00132-4](https://doi.org/10.1016/0020-7225(94)00132-4)
- [28] A.J. Omowaye, A.I. Fagbade, and A.O. Ajayi, "Dufour and soret effects on steady MHD convective flow of a fluid in a porous medium with temperature dependent viscosity: homotopy analysis approach," *J. Niger. Math.* **34**, 343–360 (2015). <https://doi.org/10.1016/j.jnnms.2015.08.001>
- [29] A. Shojaei, A.J. Amiri, S.S. Ardahaie, K. Hosseinzadeh, and D.D. Ganji, "Hydrothermal analysis of non-Newtonian second grade fluid flow on radiative stretching cylinder with Soret and Dufour effects," *Case Stud. Therm. Eng.* **13**, 100384 (2019). <https://doi.org/10.1016/j.csite.2018.100384>
- [30] H. Alfvén, Discovery of Alfvén Waves, *Nature*, **150**, 405–406 (1942). <https://doi.org/10.1038/150405d0>
- [31] T.G. Cowling, *Magnetohydrodynamics*, (Wiley Inter Science, New York, 1957).
- [32] J.A. Shercliff, *A Textbook of Magnetohydrodynamics*, (Pergamon Press, London, 1965).
- [33] K.R. Cramer, and S.I. Pai, *Magneto Fluid Dynamics for Engineers and Applied Physicists*, (Mc Graw Hill Book Co., New York, 1973).
- [34] B.K. Jha, and Y.Y. Gambo, "Unsteady free convection and mass transfer flow past an impulsively started vertical plate with Soret and Dufour effects: an analytical approach," *SN Applied Sciences*, **1**, 1234 (2019). <https://doi.org/10.1007/s42452-019-1246-1>

ТЕРМОДИФУЗІЙНИЙ ТА ДИФУЗІЙНО-ТЕРМОЕФЕКТИ НА МГД КОНВЕКТИВНИЙ ПОТІК ПОВЗ ІМПУЛЬСЬКО ЗАПУЩЕНОЮ ВЕРТИКАЛЬНОЮ ПЛАСТИНОЮ, ЗАЛОЧЕНОЮ В ПОРИСТЕ СЕРЕДОВИЩЕ

Канган Чоудхари, Світі Шарма, Шахір Ахмед

Факультет математики, Університет науки і технологій Мегхала, Індія

У цьому дослідженні представлено аналітичне рішення для нестационарної вільної МГД-конвекції та потоку масообміну повз вертикальну пластину, вбудовану в пористе середовище, з урахуванням ефектів Соре та Дюфура. Спочатку метод збурень використовується для роз'єднання рівнянь, що є результатом зв'язку ефектів Соре та Дюфура. Для розв'язання керівних рівнянь використовується метод перетворення Лапласа. Отримано вирази для швидкості, температури, концентрації, шкірного тертя, чисел Нуссельта та Шервуда. Обговорюються ефекти основних параметрів, показуючи, що збільшення числа Соре призводить до зниження температури при збільшенні швидкості та концентрації. Подібним чином параметр Дюфура викликає підвищення температури та швидкості, тоді як концентрація зменшується. Однак вплив параметрів Дюфура та Соре на швидкість не демонструє істотної різниці.

Ключові слова: МГД; ефект Соре; ефект Дюфура; збурення; перетворення Лапласа